American Journal of Astronomy and Astrophysics
2026, Vol. 13, No. 3, pp. 88–96
https://doi.org/10.11648/j.ajaa.20261303.11

SciencePG
Science Publishing Group

Research Article

Investigating Star Formation Rate, Metallicity and Mass Relations in Dwarf Galaxies

Emenike Nwaokoro*

Department of Physics, Abia State University, Uturu, Nigeria

Abstract

Star formation rate (SFR), metallicity, and mass have been identified as the key to understanding how galaxies form and evolve. To show the actual contribution of star-formation to the growth of galaxies, specific star formation rate (SSFR) is used in place of SFR. SSFR is defined as a quantity that measures the SFR per unit galaxy stellar mass. It is the measure of time taken by a galaxy to form its stellar mass at its current star formation rate. The relation between SSFR and mass separates galaxies into two populations: those with active star formation and those with little or no star formation. Metallicity is the mass fraction of baryonic components in metals; it traces the fraction of baryonic mass already converted to stars. The purpose of this paper is to present results obtained from the investigation of mass, metallicity, and star formation rate relations in dwarf galaxies using data from Sloan Digital Sky Survey matched with Galaxy and Mass Assembly. 863 emission-line classified star-forming galaxies were used for this study. Stellar mass was estimated based on an empirical relation from the (g - i) band colour. Hα luminosity was used to estimate the star formation rate (SFR). Metallicities were estimated using three methods, namely Z94, T04 and D02, which are based on theoretical methods, empirical methods and a combination of both, respectively. Results obtained showed an increase in star formation rate with mass, with a lot of scatter, which is greater among dwarf galaxies. Towards normal galaxies, the star formation rate dropped, which may be due to AGN feedback. A decreasing SSFR with mass was obtained, with dwarf galaxies having higher SSFR than normal galaxies, indicating that star formation contributes more to the growth of dwarf galaxies, thereby rapidly increasing their stellar mass more than in the normal galaxies. Also, the downsizing effect can be used to explain this observation. Generally, the results for mass-metallicity (M-Z) relations showed that for all populations, metallicity increased with mass, with increased scatter in the dwarf galaxy region. The scatter observed in the dwarf galaxy region is due to the presence of lower metallicity objects. Z94 M-Z relation has more scatter than other M-Z relations and has higher metallicities. Even though the metallicity values for my dwarf galaxies are low compared with other galaxies, they are higher than those of dwarf irregular galaxies, suggesting that my dwarf galaxy sample is dominated by dwarf galaxies with different morphologies that have high metallicity, such as dwarf spirals.

Keywords

Abundances, Evolution, Star Formation, Dwarf Galaxies

*Correspondence: Emenike Nwaokoro (nwaokoro.emenike@abiastateuniversity.edu.ng)

Received: 8 June 2026; **Accepted:** 22 June 2026; **Published:** 22 July 2026

1. Introduction

Star formation rate (SFR), metallicity, and mass have been identified as the key to understanding how galaxies form and evolve [4, 5, 13, 18, 19]. Dwarf galaxies are low luminosity and low mass galaxies. They have absolute B-magnitude, M_B, fainter than -17 and stellar mass that is less than 10^{10} $M_{\odot}$. Variations in star formation rate and chemical enrichment history have been observed in dwarf galaxies and the mechanisms responsible for these variations are still being studied even to higher redshift (e.g. [7, 25, 31]). Galaxies at high redshifts have been observed to have lower metallicity compared to similar sized galaxies at low redshift.[21]. Supernova feedback and the interaction between dwarf galaxies and their bigger cousins have been suggested as mechanisms that regulate star formation, gas and metal content [28, 29]. Late-type dwarf galaxies are more consistent in their star formation over a long period (even till present day) with short intervals of inactivity and at different rates [31]. Their ability to sustain star formation is due to the presence of a large amount of gas in their interstellar medium. Early type dwarf galaxies have little or no gas content, therefore, are mainly made up of old stars and have shown no recent star formation with the exception of NGC 205, Antlia, NGC 185 [25] and some Virgo cluster early-type dwarf galaxies that have blue central regions, indicating on going or star formation activities [23]. The colour magnitude diagram and star formation history of some early type dwarfs (e.g. Carina and Fornax dSphs) show that they have experienced intense star formation at different times [25, 31] probably due to close interaction with bigger galaxies.

To show the actual contribution of star-formation to the growth of galaxies, specific star formation rate (sSFR) is used in place of SFR [4]. SSFR is defined as a quantity that measures the SFR per unit galaxy stellar mass [3, 25]. Its unit is an inverse of time; therefore, it is also defined as a measure of time taken by a galaxy to form its stellar mass at its current star formation rate [6]. The relations between sSFR and mass split galaxies into two, those with ongoing star formation and those with little or no star-formation called the quiescent populations, mostly the early-type galaxies.

Metallicity, as defined by [26], is the mass fraction of baryonic components in metals; it traces the fraction of baryonic mass already converted to stars [18, 19]. Star formation, infall of metal-poor gas and outflow of enriched materials processed in stars control metallicity [5]. Its correlation with mass was first observed by [20] while studying the chemical composition and evolution of star-forming galaxies. The relation between metallicity and mass have it that more massive galaxies have higher metallicity than the low mass galaxies, which has been associated to metal loss due to supernovae and stellar wind [19]. Like every other galaxy, dwarf galaxies have complex chemical enrichment and star-formation histories. Low metallicity in dwarf galaxies has been attributed to galactic winds associated with supernova explosions and ram pressure/tidal stripping [31]. These mechanisms are very effective in removing metal-rich gases from dwarf galaxies because of their shallow potential which makes unable to retain metal-rich gas during these turbulent activities, unlike their larger galaxies. Downsizing effect, as noted by [8] has been used to explain the low metallicity in low-mass galaxies. In this case, the star formation in low-mass galaxies occurs more slowly and over a longer timescale than their massive counterparts, indicating they have low star formation efficiency due to supernova activity [16, 19]. Also low star formation efficiency in dwarf galaxies due to downsizing effect has been proposed to play a role in lowering the metallicity of dwarf galaxies [19]. Other mechanisms proposed include accretion of metal poor/metal-free gas, changes in the initial mass function (IMF), steeper IMF slopes and mass range cut-offs [6, 31].

Strong optical emission lines, such as oxygen, nitrogen and sulphur, have been used as a measure of metal abundance in galaxies has become very popular among astronomers recently, for example [29, 32, 33]. [32] outlined three advantages of the use of emission lines:

1) It is not affected by uncertainties due to age and α-enhancements.
2) It has a much higher signal-to-noise ratio.
3) It is easier to interpret because it gives the present-day metallicity.

The only disadvantage of the use of strong emission lines for estimating metallicity is that it is limited to only star forming galaxies. Dwarf galaxies are mostly star-forming (HII region) galaxies and display mostly emission lines [16, 28] making it more appropriate to use emission lines to estimate metallicity for dwarf galaxies.

The purpose of this paper is to present results obtained from the investigation of mass, metallicity and star formation rate relations in dwarf galaxies using data from Sloan Digital Sky Survey matched with Galaxy And Mass Assembly.

2. Data and Sample Selection

Matched data obtained from Sloan Digital Sky Survey Data Release 12 (SDSS DR 12) [1] and Galaxy And Mass Assembly (GAMA) Survey Data Release II (DR 2) [22] was used in this study. SDSS being very large photometric and spectroscopic survey covering 10,000 deg^2 of the sky and GAMA is a multiwavelength spectroscopic survey with high spectroscopic completeness of 2 magnitude deeper than SDSS allowing the study of more dwarf galaxies. The galaxies selected from both SDSS and GAMA surveys are galaxies with absolute G magnitude, M_g, fainter than -20, a redshift range of $0.002 \leq z \leq 0.1$ (so as to remove Galactic stars) and a reliable redshift with zWarning = 0 (for SDSS data) and redshift quality, $nQ \geq 3$ (for GAMA data). Galaxies above the spectroscopic magnitude limit (r-Petrosian magnitude > 17.77 and 19.8 for SDSS and GAMA respectively) and galaxies with nuclear contamination (composite and AGN galaxies) were, also, eliminated using BPT diagram [2] (see Figure 1). Therefore, 863 emission line classified star-forming galaxies are used for this study.

3. Analysis

3.1. Selection of Star-forming Galaxies via BPT Diagram

A way of separating star-forming (SF) galaxies from those with active nuclei was provided by [2] through the use of strong emission line ratio diagrams, popularly known as BPT diagrams. These emission line ratio diagrams are [NII]λ6583/Hα and [OIII]λ5007/Hβ, [OI]λ6300/Hα and [OIII]λ5007/Hβ, [SII]λλ6717,6731/Hα and [OIII]λ5007/Hβ. Of these three diagrams the most commonly used is the [NII]λ6583/Hα and [OIII]λ5007/Hβ because with this diagram galaxies can be separated into three categories, using the relations of [16] eqn (1) and [15] eqn (2), namely star-forming, composite and AGN (active galactic nucleus) galaxies. Star-forming galaxies are galaxies which have star-forming/HII regions, they lie below the Kauffmann and Kewley line diagnostics on the BPT diagram. The composite galaxies have a mixture of the star-forming/HII regions with high metal enrichment [11] and AGN contaminations, they lie between Kauffmann and Kewley line diagnostics. They are also called Transitional objects. AGN galaxies are galaxies that have their light emission dominated by an active nucleus, they lie above Kauffmann and Kewley line diagnostics. Below are the relations of [16] and [15] for the emission line classification of galaxies.

relations for SF and AGN galaxy separation [16]:

$$\log[OIII]/H\beta = 0.61/\log([NII]/H\alpha - 0.47) + 1.19 \quad (1)$$

relations [15]:

$$\log([OIII]/H\beta) = 0.61/\log([NII]/H\alpha - 0.05) + 1.30 \quad (2)$$

Figure 1 below shows the BPT diagram for the total SDSS-GAMA matched galaxies. The red dots on the matched sample are dwarf galaxies; the solid line is the [16] relation and the dashed line is [15] relation. Star-forming galaxies are below the dashed line, composite galaxies are between the solid and dashed line and AGN galaxies are above the solid line. The galaxies used for this study are 863 emission-line classified star-forming galaxies (galaxies below the dashed line).

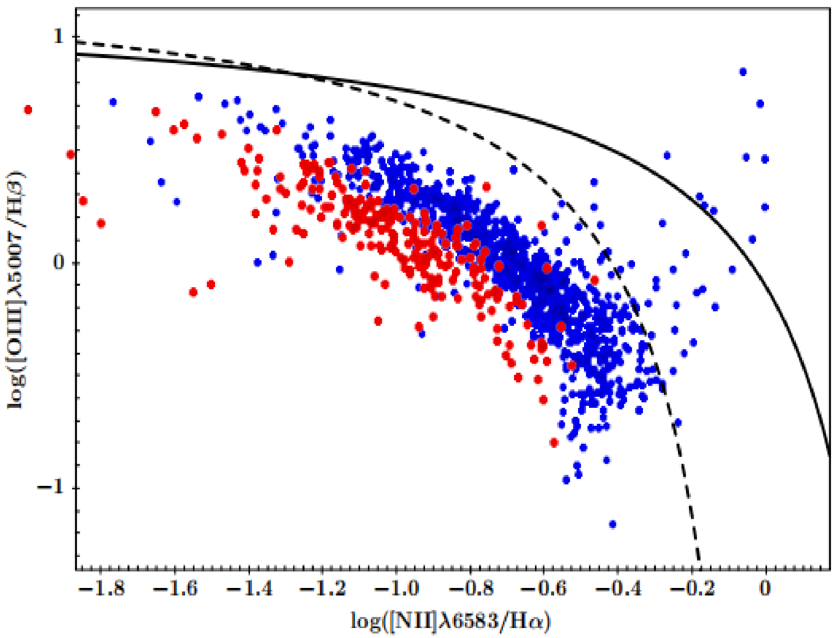

Figure 1. *BPT diagram for the total SDSS-GAMA matched galaxies. The red dots on the matched sample are dwarf galaxies; the solid line is the [16] relation and the dashed line is [15] relation.*

3.2. Stellar Masses

Stellar mass was estimated based on empirical relation provided by [30] as documented by [12], which can only be used with the (g - i) band colour.

$$\log M_* = -0.68 + 0.73(g - i) - 0.4\left(M_i - M_{i,\odot}\right) \quad (3)$$

where M_i is the i-band absolute magnitude and $M_{i,\odot}$ is the absolute magnitude of the Sun in the i-band given as 4.58. g- and i-band magnitudes are k corrected to z = 0 therefore the (g - i) colour is given by (g - k_g) - (i - k_i), where k_g and k_i are the k-corrections at g and i bands respectively.

3.3. Star Formation Rate (SFR)

We used the Hα luminosity to estimate the star formation rate (SFR) because it measures the present star formation to the last 10^6 years produced by ionizing photons from short-lived, hot and massive stars [12]. The estimated SFR is based on the approach of [14] as documented by [12] and [19]. Due to the size of the diameter of the spectroscopic fibre, which may be smaller than the source, aperture correction was made to recover the missed light and obtain the true value of the star formation rate. We also corrected for stellar absorption in the Hα equivalent width, $EW_{H\alpha}$, (Å) and dust obscuration. We used a common value of 1.3Å for the stellar absorption equivalent width correction, EW_c, as used by [12] and [14].

Below is the expression used to estimate the SFR for the galaxies classified as star forming/HII dwarf galaxies:

$$SFR_{H\alpha}(M_{\odot}yr^{-1}) = \frac{L_{H\alpha}(W)}{1.27\times10^{34}} \quad (4)$$

$$L_{H\alpha}(W) = (EW_{H\alpha} + EW_c) \times 10^{-0.4(M_r-34.10)} \times \frac{3\times10^{18}}{[6564.61(1-z)]^2} \times \left[\frac{F_{H\alpha}/F_{H\beta}}{2.86}\right]^{2.36} \quad (5)$$

where M_r is the r-band absolute magnitude, z is the redshift, $L_{H\alpha}$ is the H_α luminosity and $F_{H\alpha}/F_{H\beta}$ is the ratio of the H_α flux to the H_β flux known as the Balmer decrement (BD), which measures interstellar reddening or extinction and has a set value of 2.86 known as the Case B recombination value.

3.4. Gas Metallicity Measurements

Different metallicity calibrations based on different strong emission line ratios were described by [17]. These methods are either based on photoionization models (theoretical methods), measuring directly the electron temperature of the ionized gas (empirical methods), or both.

For our emission line classified star-forming galaxies we estimated gas metallicities using three methods, which represent the different groups.

The first method used in measuring metallicities of the galaxy samples is based on the line ratios of ([OIII]λ5007/Hβ) and ([NII]λ6583/Hα), referred to as O3N2 parameter.

$$O3N2 = \log\left(\frac{OIII\lambda5007/H\beta}{NII\lambda6583/H\alpha}\right) \quad (6)$$

The O3N2 parameter is valid for O3N2 < 2. The O3N2 parameter is calibrated using the empirical method of [27] known as the PP04 O3N2 and is given by

$$[12 + \log(O/H)]_{\mathrm{PP04}} = 8.73 - 0.32 \times \mathrm{O3N2} \quad (7)$$

Metallicity derived by empirical methods, as observed by [19], yields lower metallicity with ~ 0.3 dex offset. In order to eliminate low metallicities and offsets of empirical methods [19] derived a conversion from PP04 O3N2 method to the [32] theoretical method:

$$[12 + \log(O/H)]_{\mathrm{T04}} = 0.1026 + 1.0211 \times [12 + \log(O/H)]_{\mathrm{PP04}} \quad (8)$$

where [12+log(O/H)] is the unit of metallicity derived using oxygen abundance, PP04 and T04 refer to [27] and [32] methods, respectively. Metallicities derived using the O3N2 parameter eliminate reddening or extinction corrections and flux calibration due to the closeness of the emission line ratios [17, 19].

The second method is one of the theoretical methods, [34] calibrations known as Z94. This method relies on the ratio of [OII] and [OIII] to Hβ line, known as R_{23} given by

$$R_{23} = \frac{([OII]\lambda3727 + [OIII]\lambda\lambda5007{,}5007)}{H\beta} \quad (9)$$

The above equation results in a metallicity estimate that is either classed as an upper branch or a lower branch and the division occurs at log([NII]/[OII]) ~ -1.2 or 12 + \log(O/H) ~ 8.4 of the theoretical method. The Z94 calibration is given by

$$[12 + \log(O/H)]_{\mathrm{Z94}} = 9.265 - [0.33 \times \log \mathrm{R}_{23}] - [0.202 \times (\log \mathrm{R}_{23})^2] - [0.207 \times (\log \mathrm{R}_{23})^3] - [0.333 \times (\log \mathrm{R}_{23})^4] \quad (10)$$

This calibration is valid for the R_{23} upper branch at log([NII]/[OII]) > -1.2 or 12 + \log(O/H) > 8.4.

The third method used is the [9] method, known as D02, as described in Appendix A of [17]. This calibration is derived from metallicities based on the direct method known as the T_e method and the [NII]/Hα strong line ratio. The T_e method is based on metallicities converted from the electron temperature of a gas estimated from the ratio of [OIII]λ4363 line to the [OIII]λ5007 line or any other lower excitation line. The linear least-square fit in the relationship between these two methods for ~ 155 HII regions gave the D02 method. The calibration is given by

$$[12 + \log(O/H)]_{\mathrm{D02}} = 9.12 + 0.73 \times \log([\mathrm{NII}]/\mathrm{H}\alpha) \quad (11)$$

This calibration is valid for -2.5 < log([NII]/Hα) < -0.3.

4. Results and Discussion

4.1. Star Formation Rate and Specific Star Formation Rate - Mass Relations

Figure 2 shows the relationship between SFR and sSFR with mass. Figure 2a shows an increase in star formation rate with mass, albeit with a lot of scatter. The scatter is greater among the dwarf galaxies $M_*/M_\odot \leq 10^9$, the galaxies that move away from the steady increasing trend in the plot represent elliptical and lenticular galaxies in [24]. Towards the higher mass $M_*/M_\odot \geq 10^{10}$ the star formation rate in the galaxies drops, which means that as galaxies increase in mass their star formation rate starts going down due to AGN feedbacks.

Figure 2b shows a decreasing sSFR with mass and the dwarf galaxies having higher sSFR than the bigger galaxies, this means that star-formation contributes more to the growth of low mass galaxies therefore, they are more rapidly increasing their stellar mass than the bigger galaxies [19]. Another explanation to this, being given by [29], is the downsizing effect, the time taken for star formation is longer in dwarf or low mass galaxies than in massive galaxies.

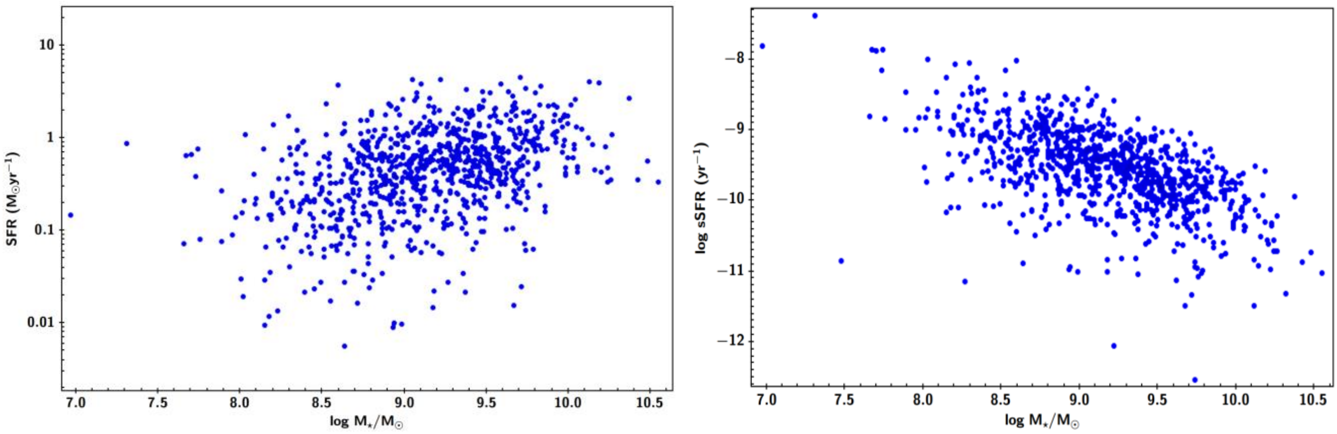

Figure 2. *The relationship between (a) SFR and (b) sSFR with mass.*

4.2. Metallicity - Mass Relations

Figure 3 shows the mass-metallicity (MZ) relations for the three different metallicity calibrations: O3N2 parameter calibrated to T04 metallicity [32], D02 method [9] and Z94 method [34], the metallicities values are solar $Z_\odot$. For the mass-metallicity plots, the number of galaxies valid within the O3N2 parameter are 853 galaxies, 858 galaxies for D02 and 838 for the Z94 calibrations. The dwarf galaxies, in all the plots, have lower metallicity as described above. Also, metallicity increases with mass (as expected) and the scatter in mass-metallicity relations is greater in the low mass galaxies $M_*/M_\odot \leq 10^9$. This was also observed by [33] and suggested that this was due to the presence of lower metallicity objects. The Z94 MZ relation has more scatter than other MZ relations and has higher metallicities, as seen in the next figure. Even though the metallicity values for low mass galaxies are low compared with regular/brighter galaxies, but the values are higher than dwarf irregular galaxies, which indicates that our dwarf galaxy samples may mostly be dominated by dwarf spirals.

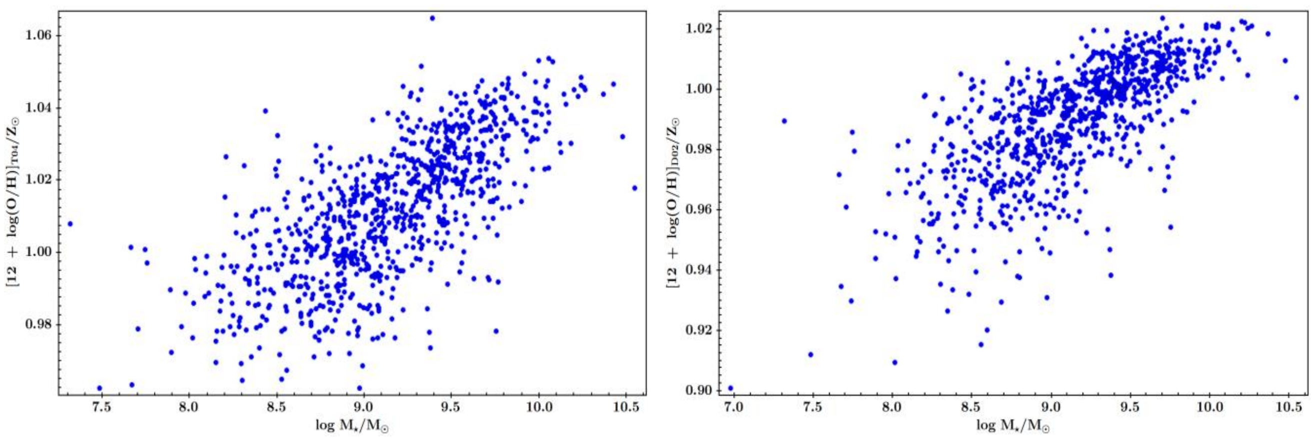

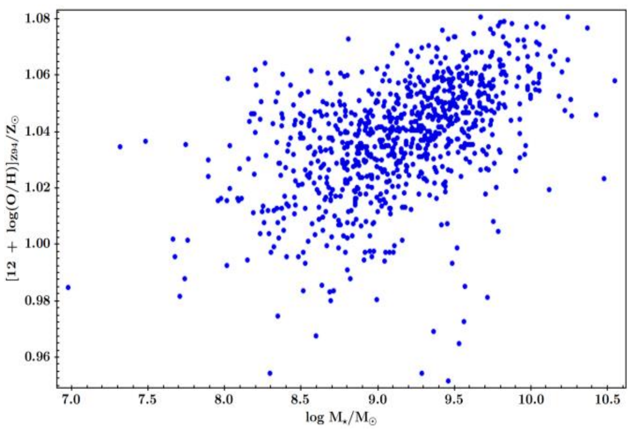

Figure 3. *Metallicity versus stellar mass plots for SDSS-GAMA matched galaxy sample using the three different calibrations: (a) T04, (b) D02 and (c) Z94 respectively. The estimated metallicity values are solar metallicities.*

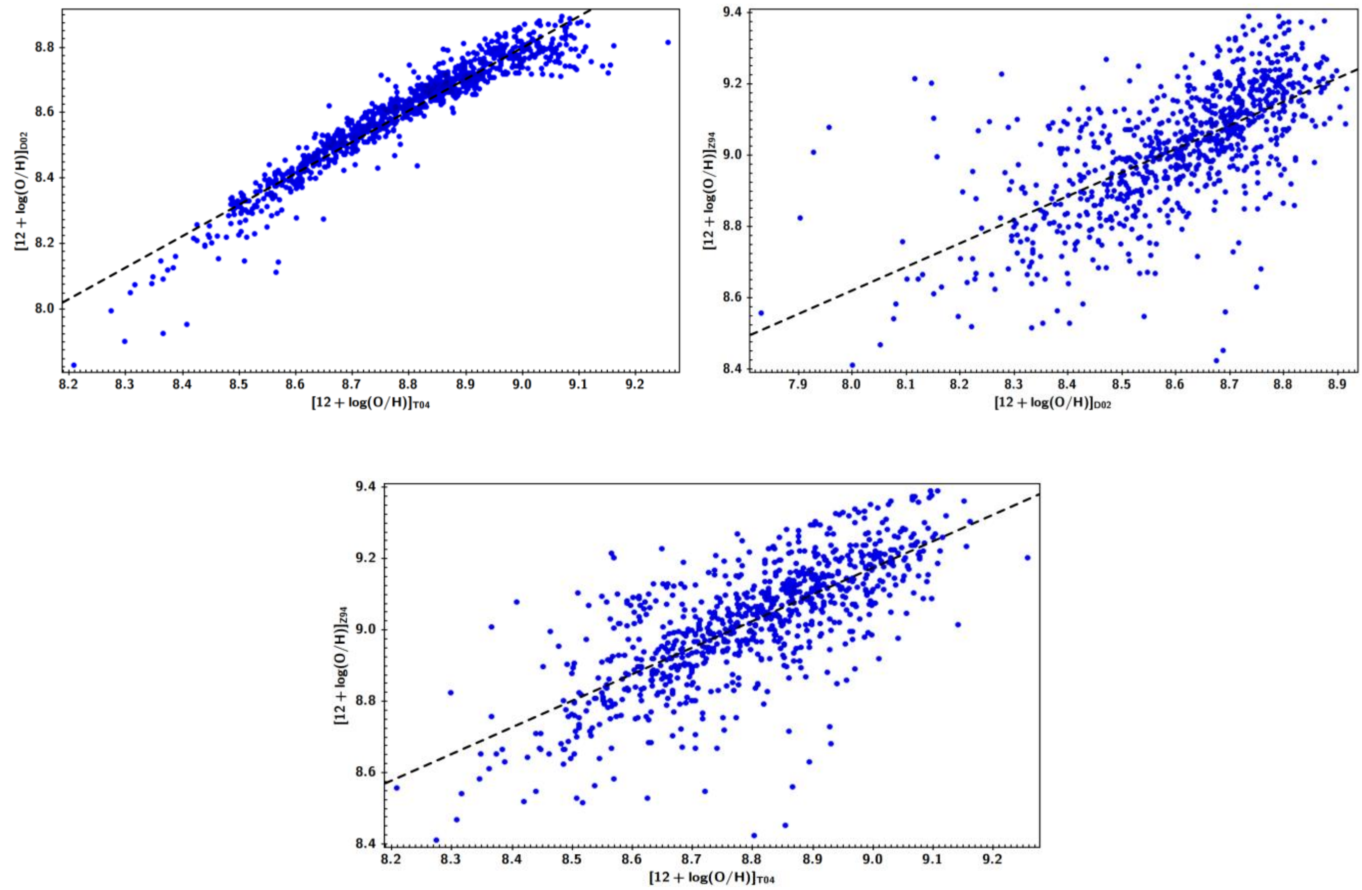

Figure 4. *Plots comparing the three different metallicity calibrations. (a) D02 versus T04, (b) Z94 versus D02 and (c) Z94 versus T04. The metallicity values are not solar.*

Figure 4 compares the different metallicity calibrations. The Z94 gives higher metallicity than other calibrations (~0.2 dex higher than T04 and 0.5 dex than D02 calibration) followed by the T04 method, which is ~0.4 dex higher than D02. The Z94 higher metallicity is expected because the calibration is a direct photoionization method and this method gives higher metallicities of about 0.3 dex above other methods. T04 also have higher metallicity but it is about 0.2 dex lower than Z94, this may be due to its conversion from the empirical method of PP04.

5. Summary and Conclusion

I have presented results obtained from the investigation of mass, metallicity, and star formation rate relations in dwarf galaxies using data from Sloan Digital Sky Survey DR 12 matched with Galaxy And Mass Assembly DR 2. 863 emission-line classified star-forming galaxies were used for this study. Stellar mass was estimated based on empirical relation from the (g - i) band colour. Hα luminosity was used to estimate the star formation rate (SFR). Metallicities were estimated using three methods, namely Z94, T04 and D02, which are based on theoretical methods, empirical methods, and a combination of both, respectively. Results obtained showed an increase in star formation rate with mass, with a lot of scatter, which is greater in the dwarf galaxy region. Towards normal galaxies, the star formation rate dropped, which may be attributed to AGN feedback. A decreasing sSFR with mass was obtained, with dwarf galaxies having higher sSFR than normal galaxies, indicating that star formation contributes more to the growth of dwarf galaxies, thereby rapidly increasing their stellar mass than in the bigger galaxies. Also, the downsizing effect can be used to explain this observation. Generally, the results for mass-metallicity (M-Z) relations showed that for all populations, metallicity increased with mass, with increased scatter and low metallicity in dwarf galaxies. This is due to the presence of lower metallicity objects. The low metallicity observed in dwarf galaxies may be due to metal loss caused by highly energetic activities associated with star formation or the downsizing effect. Z94 M-Z relation has more scatter and has higher metallicity value than other M-Z relations (~0.2 dex higher than T04 and 0.5 dex than D02 calibration) followed by the T04 method, which is ~0.4 dex higher than D02. This is in agreement with [10]. Z94 higher metallicity is expected because the calibration is a direct photoionization method and this method gives higher metallicities of about 0.3 dex above other methods [10]. Even though the metallicity values for my dwarf galaxy samples are low compared with other galaxies, the values are higher for dwarf irregular galaxies. With SDSS being very large photometric and spectroscopic survey and GAMA a multiwavelength spectroscopic survey with high spectroscopic completeness of 2 magnitudes deeper than SDSS my future research will to investigate the different morphologies of the dwarf galaxies in my sample. I will, also, probe into the actual reason for the observed low metallicity in my dwarf galaxy samples.

Abbreviations

SDSS	Sloan Digital Sky Survey
GAMA	Galaxy And Mass Assembly
DR	Data Release
NGC	New General Catalogue of Nebulae and Clusters of Stars
T04	Tremonti Et Al. (2004)
Z94	Zarisky Et Al 1994
D02	Denicolό 2002
PP04	Pettini and Pagel 2004
MZ	Mass-metallicity Relations
SF	Star Forming
SFR	Star Formation Rate
sSFR	Specific Star Formation Rate
BPT	Baldwin, Phillipps and Terlevich
AGN	Active Galactic Nuclei
Hα	Hydrogen Alpha Line
Hβ	Hydrogen Beta Line
EWHα,	Hydrogen Alpha Equivalent Width
λ	Wavelength
HII	Hydrogen 2 Emission Line
[OI]λ6300	Oxygen 1 Emission Line
[OII]	Oxygen 2 Emission Line
[OIII] or [OIII]λ5007	Oxygen 3 Emission Line
[NII] or [NII]λ6583	Nitrogen 2 Emission Line
[SII]λλ6717,6731	Sulphur 2 Emission Line Wavelengths 6717 and 6731
Te	Electron Temperature
MB	Absolute B-magnitude
Mg	Absolute G-magnitude
MΘ	Solar Mass
z	Redshift
nQ	Redshift Warning
R23	The Ratio of [OII] and [OIII] to Hydrogen Beta Line
Mi	I-band Absolute Magnitude
$Mi,_{\odot}$	Absolute Magnitude of the Sun in the I-band
[12+log(O/H)]	The Unit of Metallicity Derived Using Oxygen Abundance
Dex	Decimal exponent

Author Contributions

Emenike Nwaokoro: Conceptualization, Data curation, Investigation, Methodology, Resources, Writing – original draft

Conflicts of Interest

The author declares no conflict of interest.

References

[1] Alam, S., Albareti, F. D., Allende P. C., Anders, F., Anderson, S. F., Anderton, T., Andrews, B. H., Armengaud, E., Aubourg, É., Bailey, S., Basu, S., Bautista, J. E., Beaton, R. L., Beers, T. C., Bender, C. F., Berlind, A. A., Beutler, F., Bhardwaj, V., Bird, Jonathan C., …, Zhu, G. (2015). The Eleventh and Twelfth Data Releases of the Sloan Digital Sky Survey: Final Data from SDSS-III. *The Astrophysical Journal Supplement Series*, 219(1), 27. https://doi.org/10.1088/0067-0049/219/1/12

[2] Baldwin, J. A., Phillips, M. M. & Terlevich, R. (1981). Classification parameters for the emission-line spectra of extragalactic objects. *Publications of the Astronomical Society of the Pacific*, 93(551), 5-19. https://doi.org/10.1086/130766

[3] Bauer, A. E., Drory, N. & Hill G. J. (2006). Specific star formation rates. In LeBrun V., Mazure A., Arnouts S., Burgarella D., (Eds). The Fabulous Destiny of Galaxies: Bridging Past and Present. Paris: Frontier Group, p. 279. https://doi.org/10.48550/arXiv.astro-ph/0509059

[4] Bidaran B., Puertas S. D., Pérez I., Zurita A., Espada D., Argudo-Fernández M., García-Benito R., Sánchez-Menguiano R., Verley S., Sánchez S. F., Falcón-Barroso J., Ferré-Mateu A., Villalba-Gonzalez P., Jiménez A., Peletier R. F., Ruiz-Lara T. (2026). The Gas-Phase Mass-Metallicity Relation of Dwarf Galaxies Across Large-Scale Environments Using the CAVITY Parent Sample. *Astronomy & Astrophysics*. https://doi.org/10.48550/arXiv.2605.25557

[5] Bulichi, T., Fahrion, K., Mernier, F., Hilker, M., Leaman, R., Lyubenova, M., Müller, O., Neumayer, N., Martin-Navarro, I., Pinna, F., Rejkuba, M., Scholz-Diaz, L. & van de Ven, G. (2023). Expanding on the fundamental metallicity relation in dwarf galaxies with MUSE. *Astronomy & Astrophysics*. 679, A98. https://doi.org/10.1051/0004-6361/202346002

[6] Ciambur, B. C., Kauffmann, G. & Wuyts, S. (2013). On the evolution of the bi-modal distribution of galaxies in the plane of specific star formation rate versus stellar mass. *Monthly Notices of the Royal Astronomical Society*, 432(3), 2488 - 2495. https://doi.org/10.1093/mnras/stt631

[7] Curti M., Maiolino R., Curtis-Lake E., Chevallard J., Carniani S., D'Eugenio F., Looser T. J., Scholtz J., Charlot S., Cameron A., Übler H., Witstok J., Boyett K., Laseter I., Sandles L, Arribas S., Bunker A., Giardino G., Maseda M. V… Sun F. (2024). JADES: Insights into the low-mass end of the mass-metallicity-SFR relation at $3 < z < 10$ from deep JWST/NIRSpec spectroscopy. *Astronomy & Astrophysics*. 684, A75. https://doi.org/10.1051/0004-6361/202346698

[8] Cowie L. L., Songaila A., Hu E. M., Cohen J. G. (1996). New Insight on Galaxy Formation and Evolution From Keck Spectroscopy of the Hawaii Deep Fields. *Astronomical Journal*, 112, 839. https://doi.org/10.48550/arXiv.astro-ph/9606079

[9] Denicoló, G., Terlevich, R. & Terlevich, E. (2002). New light on the search for low-metallicity galaxies - I. The N2 calibrator. *Monthly Notices of the Royal Astronomical Society*, 330(1), 69-74. https://doi.org/10.1046/j.1365-8711.2002.05041.x

[10] Foster, C., Hopkins, A. M., Gunawardhana, M., Lara-López, M. A., Sharp, R. G., Steele, O., Taylor, E. N., Driver, S. P., Baldry, I. K., Bamford, S. P., Liske, J., Loveday, J., Norberg, P., Peacock, J. A., Alpaslan, M., Bauer, A. E., Bland-Hawthorn, J. Brough, S., Cameron, E.,… Wijesinghe, D. (2012). Galaxy And Mass Assembly (GAMA): the mass-metallicity relationship. *Astronomy & Astrophysics*, 547, A79, 9 pp. https://doi.org/10.1051/0004-6361/201220050

[11] Groves B., Kewley L. (2008). Distinguishing Active Galactic Nuclei and Star Formation. In Knapen J. H., Mahoney T. J., Vazdekis A. (Eds). *Pathways Through an Eclectic Universe*. Astronomical Society of the Pacific Conference Series. 390, 283. https://doi.org/10.48550/arXiv.0707.0158

[12] Gunawardhana, M. L. P., Hopkins, A. M., Sharp, R. G., Brough, S., Taylor, E., Bland-Hawthorn, J., Maraston, C., Tuffs, R. J., Popescu, C. C., Wijesinghe, D., Jones, D. H., Croom, S., Sadler, E., Wilkins, S., Driver, S. P., Liske, J., Norberg, P. Baldry, I. K., Bamford, S. P., …van Kampen, E. (2011). Galaxy and Mass Assembly (GAMA): the star formation rate dependence of the stellar initial mass function. *Monthly Notices of the Royal Astronomical Society*, 415(2), 1647-1662. https://doi.org/10.1111/j.1365-2966.2011.18800.x

[13] Hansson, K. S. A., Lisker, T., & Grebel, E. K., (2012). Observed versus modelled u-, g-, r-, i-, z-band photometry of local galaxies - evaluation of model performance. *Monthly Notices of the Royal Astronomical Society*. 427(3), 2376-2391. https://doi.org/10.1111/j.1365-2966.2012.21659.x

[14] Hopkins, A. M., Miller, C. J., Nichol, R. C., Connolly, A. J., Bernardi, M., Gómez, P. L., Goto, T., Tremonti, C. A., Brinkmann, J., Ivezić, Ž. & Lamb, D. Q. (2003). Star Formation Rate Indicators in the Sloan Digital Sky Survey. *The Astrophysical Journal*, 599(2), 971 - 991. https://doi.org/10.1086/379608

[15] Kauffmann, G., Heckman, T. M., Tremonti, C., Brinchmann, J., Charlot, S., White, S. D. M., Ridgway, S. E., Brinkmann, J., Fukugita, M., Hall, P. B., Ivezić, Ž., Richards, G. T. & Schneider, D. P. (2003). The host galaxies of active galactic nuclei. *Monthly Notices of the Royal Astronomical Society*, 346(4), 1055-1077. https://doi.org/10.1111/j.1365-2966.2003.07154.x

[16] Kewley, L. J., Dopita, M. A., Sutherland, R. S., Heisler, C. A., & Trevena, J. (2001) Theoretical modeling of starburst galaxies. *The Astrophysical Journal*, 556(1), 121 - 140. https://doi.org/10.1086/321545

[17] Kewley L. J. & Ellison S. L. (2008). Metallicity Calibrations and the Mass-Metallicity Relation for Star-forming Galaxies. AJ, 681, 1183 - 1204. https://doi.org/10.1086/587500

[18] Lara-López, M. A., Bongiovanni, A., Cepa, J., Pérez García, A. M. Sánchez-Portal, M., Castañeda, H. O., Fernández Lorenzo, M. & Pović, M. (2010). Study of star-forming galaxies in SDSS up to redshift 0.4. II. Evolution from the fundamental parameters: mass, metallicity and star formation rate. *Astronomy & Astrophysics*, 519, A31. https://doi.org/10.1051/0004-6361/200913886

[19] Lara-López, M. A., Hopkins, A. M., López-Sánchez, A. R., Brough, S., Gunawardhana, M. L. P., Colless, M., Robotham, A. S. G., Bauer, A. E., Bland-Hawthorn, J., Cluver, M., Driver, S., Foster, C., Kelvin, L. S., Liske, J., Loveday, J., Owers, M. S., Ponman, T. J., Sharp, R. G., Steele, O., …. Thomas, D. (2013). Galaxy And Mass Assembly (GAMA): a deeper view of the mass, metallicity and SFR relationships. *Monthly Notices of the Royal Astronomical Society*, 434 (1), 451 - 470. https://doi.org/10.1093/mnras/stt1031

[20] Lequeux J., Peimbert M., Rayo J. F., Serrano A., Torres-Peimbert S. (1979). Chemical composition and evolution of irregular and blue compact galaxies. *Astronomy & Astrophysics*, 80, 155-166. https://ui.adsabs.harvard.edu/abs/1979A&A.80.155L

[21] Li M., Cai Z., Bian F., Lin X., Li Z., Wu Y., Sun F., Zhang S., Golden-Marx E., Sun Z, Zou S., Fan X., Egami E., Charlot S., Bruzual G., Chevallard J. (2023). The mass-metallicity relation of dwarf galaxies at cosmic noon from jwst observations. *The Astrophysical Journal Letters*. 955, L18 (14pp). https://doi.org/10.3847/2041-8213/acf470

[22] Liske, J., Baldry, I. K., Driver, S. P., Tuffs, R. J., Alpaslan, M., Andrae, E., Brough, S., Cluver, M. E., Grootes, M. W., Gunawardhana, M. L. P., Kelvin, L. S., Loveday, J., Robotham, A. S. G., Taylor, E. N., Bamford, S. P., Bland-Hawthorn, J., Brown, M. J. I. Drinkwater, M. J., Hopkins, A. M., … Wright, A. H. (2015). Galaxy And Mass Assembly (GAMA): end of survey report and data release 2. *Monthly Notices of the Royal Astronomical Society*, 452, (2), 2087-2126. https://doi.org/10.1093/mnras/stv1436

[23] Lisker, T., Glatt, K., Westera, P., & Grebel, E. K., (2006). Virgo Cluster Early-Type Dwarf Galaxies with the Sloan Digital Sky Survey. II. Early-Type Dwarfs with Central Star Formation. *The Astrophysical Journal*, 132, 2432-2452. https://doi.org/10.1086/508414

[24] Mahajan S., Drinkwater M. J., Driver S., Kelvin L. S., Hopkins A. M., Baldry I., Phillipps S., Bland-Hawthorn J., Brough S., Loveday J., Penny S. J., & Robotham A. S. J. (2015). Galaxy And Mass Assembly (GAMA): the unimodal nature of the dwarf galaxy population. *Monthly Notices of the Royal Astronomical Society*, 446 (3), 2967-2984. https://doi.org/10.1093/mnras/stu2009

[25] Mateo, M., (1998). Dwarf galaxies in the Local Group. *Annual Review Astronomy and Astrophysics*, 36, 435-506. https://doi.org/10.1146/annurev.astro.36.1.435

[26] Mo, H., van den Bosch, F. C., & White, S. (2010). Galaxy Formation and Evolution. Cambridge University Press.

[27] Pettini, M. & Pagel, B. E. J. (2004). [OIII]/ [NII] as an abundance indicator at high redshift. *Monthly Notices of the Royal Astronomical Society*, 348(3), L59 - L63. https://doi.org/10.1111/j.1365-2966.2004.07591.x

[28] Phillipps S., (2005). The Structure and Evolution of Galaxies. Wiley-VCH.

[29] Sánchez-Janssen, R., Amorín, R., García-Vargas, M., Gomes, J. M., Huertas-Company, M., Jiménez-Esteban, F., Mollá, M., Papaderos, P., Pérez-Montero, E., Rodrigo, C., Sánchez Almeida, J., & Solano, E., (2013). A Virtual Observatory Census to Address Dwarfs Origins (AVOCADO). I. Science goals, sample selection, and analysis tools. *Astronomy & Astrophysics*, 554. A20. https://doi.org/10.1051/0004-6361/201219842

[30] Taylor, E. N., Hopkins, A. M., Baldry, I. K., Brown, M. J. I., Driver, S. P., Kelvin, L. S., Hill, D. T., Robotham, A. S. G., Bland-Hawthorn, J., Jones, D. H., Sharp, R. G., Thomas, D. Liske, J., Loveday, J., Norberg, P., Peacock, J. A., Bamford, S. P. Brough, S., Colless, M., … Wijesinghe, D. (2011). Galaxy And Mass Assembly (GAMA): stellar mass estimates. *Monthly Notices of the Royal Astronomical Society*, 418(3), 1587-1620. https://doi.org/10.1111/j.1365-2966.2011.19536.x

[31] Tolstoy, E., Hill, V., Tosi. M. (2009). Star-Formation Histories, Abundances, and Kinematics of Dwarf Galaxies in the Local Group. *Annual Review Astronomy and Astrophysics*, 47, 371-425. https://doi.org/10.1146/annurev-astro-082708-101650

[32] Tremonti, C. A., Heckman, T. M., Kauffmann, G., Brinchmann, J., Charlot, S., White, S. D. M., Seibert, M., Peng, E. W., Schlegel, D. J., Uomoto, A., Fukugita, M. & Brinkmann, J. (2004). The Origin of the Mass-Metallicity Relation: Insights from 53,000 Star-forming Galaxies in the Sloan Digital Sky Survey. *The Astrophysical Journal*, 613, 898 - 913. https://doi.org/10.1086/423264

[33] Zahid H. J., Bresolin F., Kewley L. J., Coil A. L. & Davé, R., (2012). The Metallicities of Low Stellar Mass Galaxies and the Scatter in the Mass-Metallicity Relation. *The Astrophysical Journal*, 750, 120 - 136. https://doi.org/10.1088/0004-637X/750/2/120

[34] Zaritsky D., Kennicutt Jr. R. C., Huchra J. P. (1994). H II regions and the abundance properties of spiral galaxies. *The Astrophysical Journal*, 420, 87 - 109. https://doi.org/10.1086/173544